# Variation in root morphology amongst tree species influences soil hydraulic conductivity and macroporosity

Webb, Bid; Robinson, David; Marshall, Miles; Ford, Hilary; Pagella, Tim; Healey, John; Smith, Andy

**Geoderma**

*DOI:*
10.1016/j.geoderma.2022.116057

Published: 01/11/2022

Peer reviewed version

# Variation in root morphology amongst tree species influences soil hydraulic conductivity and macroporosity

Bid Webb[1]*, David A. Robinson[2], Miles R. Marshall[1], Hilary Ford[1], Tim Pagella[1], John R. Healey[1], Andrew R. Smith[1]

[1]School of Natural Sciences, Bangor University, Bangor, LL57 2DG, United Kingdom

[2]UK Centre for Ecology and Hydrology, Environment Centre Wales, Deiniol Rd, Bangor, LL57 2UW, United Kingdom

*Corresponding author email: bid.webb@bangor.ac.uk

## Abstract

Natural approaches to flood risk management are gaining interest as sustainable flood mitigation options. Targeted tree planting has the potential to reduce local flood risk, however attention is generally focused on the hydrological impacts of catchment afforestation linked to generic tree features, whilst the species-specific impacts of trees on soil hydrology remain poorly understood. This study compared effects of different tree species on soil hydraulic properties. Monocultures of *Alnus glutinosa (*common alder*)*, *Fraxinus excelsior* (European ash), *Fagus sylvatica* (European beech), *Betula pendula* (silver birch), *Castanea sativa* (sweet chestnut), *Quercus robur* (English oak) and Acer *pseudoplatanus* (sycamore maple) were used to determine effects of tree species identity on soil hydraulic properties (near-saturated K and soil water retention) in a sandy loam soil, North Wales, United Kingdom. The interaction of *F. excelsior* root properties and soil class on hydraulic conductivity was also examined in four different soils (Rendzic Leptosol, Haplic Luvisol, Dystric Fluvic Cambisol and Dystric Gleysol) across England and Wales. Fine root biomass (FRB) and morphological characteristics were determined at three depths (0-0.1, 0.1-0.2 and 0.2-0.3 m) and complemented by *in situ* surface measurement of soil hydraulic conductivity. Root morphological traits were closely associated with species identity and pore-size distribution, and FRB was strongly correlated with soil hydraulic conductivity ($R^2$=0.64 for 0-0.1 m depth FRB; $R^2$=0.69 for 0.1-0.2 m depth FRB). Fine root biomass of *F.*

*excelsior* was six-fold greater than *C. sativa* ($p$<0.001), and the frequency of 0.01 mm radius soil pores under *F. excelsior* was twice that of *Q. robur*. Near-saturated hydraulic conductivity under *F. excelsior* was 7.91 ± 1.23 cm $day^{-1}$, double the mean rate of the other species. Soil classification did not significantly influence FRB ($p$ = 0.056) or near-saturated hydraulic conductivity ($p$ = 0.076) in the 0.0-0.1 m depth soil, but soil water retention varied with depth. Species-specific traits of trees should be considered in landscape design to maximise the local hydrological benefits of trees.

Keywords: Land use; Infiltration;; *Hymenoscyphus fraxineus*; Hydrology; Soil porosity; Soil classification.

## 1. Introduction

Anthropogenic activities are driving an acceleration of climate change and, as a result, the occurrence and intensity of extreme weather events is predicted to increase (IPCC5 WGII, 2014). Precipitation in the United Kingdom (UK) over the past 250 years has increased during the winter and decreased during the summer (Dadson et al., 2017). Climate change has motivated greater attention to mitigating the impact of extreme events, such as flooding, with a policy focus on the role land use management can play (Mcintyre and Thorne, 2013).

Trees have the potential to influence soil hydrological processes by increasing water infiltration into soil, evapotranspiration, interception and groundwater recharge (Dadson et al., 2017; Dixon et al., 2016; Lane, 2017; Wolton et al., 2014). Plot-scale research has notably found that even when young (5-years-old), trees can increase infiltration rate by 67 times and reduce surface runoff by 78% compared with grazed pasture (Marshall et al., 2013), but heterogeneity of effects on hydraulic conductivity at plot scale is also evident (Chandler and Chappell, 2008). The interplay between soil and vegetation shapes soil hydraulic functions, but the relative importance of these functions is context specific. In arid zones, vegetation is highly influential in increasing hydraulic conductivity (Thompson et al., 2010), whereas soil class dominates the process in humid tropical and temperate (Geris et al., 2015) ecosystems. In contrast, soil classification has generally been shown to have little effect on

infiltration capacity, with interactions between soil fauna (e.g., earthworms), roots, plant species richness and soil structure of greater importance (Fischer et al., 2015; Jarvis et al., 2013).

The role of tree roots in shaping hydraulic response has often been overlooked (Chandler et al., 2018). Understanding of inter- and intra-species variation in root morphology is largely based on the questionable assumption that root architecture and hydrological function can be predicted from above-ground morphological characteristics (Sinacore et al., 2017). Therefore, a more thorough investigation of species-specific, below-ground hydrological function is required. Macropores within soil can be associated with root channels developed through the process of root production and turnover, and enable preferential flow (Ghestem et al., 2011). Bioturbation from soil flora and fauna can also increase porosity and hydraulic function, the effects of which are influenced by landuse intensity and antecedent soil conditions, such as pH (Spurgeon et al., 2013). Preferential flow in wooded ecosystems has been shown to be related to tree species; Luo et al. (2019) reported that coniferous forests dominated by *Platycladus orientalis* (L.) Franco (oriental arbo-vitae) exhibited greater preferential flow than deciduous forests dominated by *Quercus variabilis* Blume (Chinese cork oak). Separately, a positive relationship ($R^2$ = 0.91) was identified between macroporosity and tree roots of *Pinus coulteri* D.Don (Coulter pine), but total porosity (and near-saturated conductivity) was greater under *Quercus dumosa* Nutt. (California scrub oak) and *Adenostoma fasciculatum* Hook. & Arn. (chamise), where conditions were more conducive to macrofaunal (e.g., earthworm) activity (Johnson-Maynard et al., 2002). Luo et al. (2019) reported that whilst tree roots were strongly associated with macropore development and preferential flow, the interaction between macroporosity, total porosity and infiltration was less clear. Soil total porosity and infiltration rate can have a positive relationship (Sun et al., 2018), however Bodner et al. (2014) attributed an increase in infiltration to an increase in macroporosity in soil where total porosity remained unchanged. Inconsistent effects describing the relationships between total porosity, macroporosity, preferential flow and tree species identity implies that more research is required to understand these associations.

77 Preferential flow in the vadose zone mediates water infiltration and is associated with macropores,
78 including artificial drainage (Bathurst et al., 2018; Marshall et al., 2009), macrofaunal pathways
79 (Bargues Tobella et al., 2014), biomat flow (Gerke et al., 2015) and root channels (Zhang et al., 2015).
80 However, not all fine roots are conduits for preferential flow (Luo et al., 2019), suggesting that root
81 size distribution may be more important than root biomass. For example, root length density has been
82 shown to have a strong positive correlation with preferential flow (Zhang et al., 2015) but this
83 relationship is spatially variable (Luo et al., 2019).

84 The difference in fine root production across a spectrum of the broadleaved tree species that are
85 abundant in Europe, and the consequential effect on soil hydraulic conductivity, is largely unknown.
86 Fine root production is known to be plastic, with its spatial distribution being highly responsive to
87 antecedent moisture conditions (Fan et al., 2017), which is influenced by soil texture as well as by
88 climate. Differences in hydrological response have been shown between coniferous and deciduous
89 forest ecosystems, but the response was mitigated by spatially contrasting soil texture (Luo et al.,
90 2019). The relative influence of tree species identity and soil classification on infiltration capacity
91 remains poorly understood. The aim of this study was to characterise the root morphology of seven
92 species of broadleaved, deciduous trees and investigate the relationship with near-saturated soil
93 hydraulic conductivity within one type of soil. The study then seeks to understand the effect of soil
94 classification on hydraulic conductivity in plantations of a single using tree species. The objectives
95 were to (i) investigate the variation in infiltration rate between seven tree species growing in the same
96 soil classification and (ii) compare the tree species' corresponding root morphological characteristics
97 to determine whether soil hydraulic function depends on species' root characteristics, then (iii) to
98 investigate the relative influence of tree roots and soil classification on soil hydraulic function. We
99 hypothesise that (i) tree species affect soil hydraulic conductivity; (ii) tree species' growing on the
100 same soil differ in their production of fine root biomass (FRB) and infiltration rate; and (iii) soil
101 classification affects the soil hydraulic function associated with the abundant European tree species
102 *Fraxinus excelsior* L (European ash).

## 2. Methods

### *2.1 Site descriptions and experimental design*

The BangorDiverse forest diversity and ecosystem function experiment, located at the Henfaes Research Centre, Abegwyngregyn, UK (53°14'15''N, 4°1'4''W), was used to determine the effect of tree species on soil hydraulic function. Monocultures of seven tree species were planted as 1.0 m tall saplings in March 2004: *Alnus glutinosa* [L.] Gaertner (common alder)*, F. excelsior, Fagus sylvatica* L. (European beech), *Betula pendula* Roth. (silver birch)*, Castanea sativa* Mill (sweet chestnut)*, Quercus robur* L (English oak) and *Acer pseudoplatanus* L. (sycamore maple) (Ahmed et al., 2016). Initial planting density was 10,000 stems $ha^{-1}$, but trees were thinned to 2,500 stems $ha^{-1}$ in 2012/2013 to facilitate continued tree development. Randomised, replicate plots (0.1 ha) of each species (n=4) were blocked across two adjacent fields (2.36 ha total area). The soil at BangorDiverse is a Dystric Fluvic Cambisol, developed from glaciofluvial deposits (Smith et al., 2013) with pH ranging from 5.4 (surface) to 6.3 (1-m depth) (Ahmed et al., 2016). Soil texture is a sandy loam/loam determined by laser diffraction (Coulter LS particle size analyser) from soil in the 0-0.1 m depth. The site is hyperoceanic with mean annual rainfall of approximately 950 mm and mean annual air temperature of 10.6 °C (Gunina et al., 2017).

Plots of *F. excelsior* planted in different sites across the UK with four contrasting soil classifications (IUSS Working Group WRB, 2015) were used to investigate how interaction of a single tree species with soil classification influences soil hydraulic function. Originally established as part of a provenance trial in 1993 (Cundall et al., 2003), three sites, Gloucestershire (England), Hampshire (England) and Gwynedd (Wales), were selected based on the soil classifications (Table 1) that best represented the range of textural characteristics (sand, silt or clay) commonly occurring across the UK. Each experimental site consisted of three fully replicated, randomised blocks of different provenances of *F. excelsior*. Saplings (same age from seed) were planted at 2500 stems $ha^{-1}$ and had subsequently been thinned to 50% density at the Gloucestershire site only. One plot from each block (n=3) comprised of

*F. excelsior* trees of UK (Powys, Shropshire) or French (Normandy) provenance were selected for study. Due to the presence of the fungal pathogen *Hymenoscyphus fraxineus* at the Hampshire site only, plots were selected where only visibly healthy trees were found following condition assessment (SI 1).

To increase the diversity of soils used in this analysis (Table 1), an additional site with *F. excelsior* (provenance unknown) established in 1987 at Rothamsted Research, North Wyke, Devon (England) was selected. At North Wyke, three plots were randomly selected from two blocks, avoiding edge trees. All plots were planted with seedlings at 2500 stems $ha^{-1}$ and had not been thinned. No obvious signs of *H. fraxineus* were present at North Wyke.

### *2.2 Root morphology*

Two soil cores of 0.08-m diameter were collected from three depths (0-0.1, 0.1-0.2, 0.2-0.3 m) equidistant between two trees randomly selected near to the centre of each plot to mitigate against edge effects (SI 2). Roots were collected to a depth of 0.3 m; in soil above this depth, in temperate forest ecosystems, 65% of roots exist and there is a predominance of fine ephemeral roots involved in nutrient and water uptake (Jackson et al. 1996). To minimise canopy damage and variation introduced by root growth during the sampling period, 168 samples were collected between January and February, after leaf fall and during a period of dormancy in line with previous sampling campaigns conducted at the site (Smith et al., 2013). Soil cores were placed into sealable polythene bags and stored at 4 °C for a maximum of 4 days before processing.

Each core was washed with water in a sieve stack (1- and 2-mm mesh size) to remove soil adhered to roots and separate roots into two size classes, fine (<2 mm diameter (ø)) and coarse (>2 mm ø), the latter of which were discarded. Tree species identity of the roots was based on morphological characteristics, such as surface colour, structure and colour of the periderm and ramification pattern, outlined by Mrak and Gricar (2016) and necromass (dead fine roots) was identified based on black or dark brown colour and a decaying fragmented appearance (Eissenstat and Yanai, 1997; Leuschner et

al., 2004 ; Smith et al., 2013). Fine roots were scanned using an Epson 4990 scanner at a resolution of 300 dots per inch (dpi) and images were analysed with WinRhizo (version 2005c, Regent Instruments Inc., Quebec, Canada) to measure fine root length, surface area, surface volume, projected surface area and number of root tips, divided into 20 (0.1 mm) diameter classes (0-2 mm). Necromass and the biomass of fine and coarse roots were determined after drying at 80 °C until constant mass. Data from the two soil cores collected per plot were averaged to avoid within-plot pseudoreplication.

### *2.3 Root characteristics*

Root area index (RAI, $m^2\ m^{-2}$) was derived from the root surface area divided by the surface area of the sampled core. Specific root area (SRA, $m^2\ kg^{-1}$) was calculated from the surface area of fine root divided by root dry mass (Lohmus et al., 1989). Specific root length (SRL, $m\ g^{-1}$) was determined from the total length of fine roots divided by root dry mass (Ostonen et al., 2007). Root length density (RLD, $cm\ cm^{-3}$), which indicates the proportion of soil occupied by fine roots, was estimated from the ratio of root length to the volume of the sampled core. Root tip density (RTD) was calculated as thousands of tips per $m^{-2}$. For each of the aforementioned root metrics an arithmetic mean was calculated from data exported from WinRhizo output.

### *2.4 Soil hydraulic function*

Minidisk infiltrometers (0.045 m ø) (Meter Group, Pullman, USA) were used to measure the rate of infiltration of water into soil and to calculate near-(field)-saturated hydraulic conductivity ($K_{fs}$) within each plot. Surface vegetation was carefully removed, and a thin layer of fine sand (~0.001 m) was applied to the soil surface to ensure optimal contact between the infiltrometer disc and the soil. The tension was set at -0.02 m to eliminate water flow through the largest macropores (> 0.742 mm), to provide a more representative estimation of water flow through the soil matrix and to achieve steady-state infiltration rate. Water level was recorded every minute until 20 $cm^3$ of water had infiltrated the soil. Three measurements were taken at each plot to give an average $K_{fs}$. Near-saturated hydraulic

conductivity for the respective soil water potential was calculated using the method of Zhang (1997) and van Genuchten soil classification tables (Meter Group Inc, 2018).

At each plot, a 250 $cm^3$ soil core was collected from the 0-0.05 m and 0.1-0.15 m depths. Cores were stored at 4 °C and then soaked for at least 24 hours in degassed, deionised water prior to analysis. Soil water retention was measured using a HYPROP 2 (Meter group, Pullman, USA) (Schindler et al., 2010), and then dry bulk density and porosity were determined for the cores (SI 3). To account for the stoniness of the experimental plots, stones (>0.002 m ø) were sieved out of the oven-dried soil and weighed (SI 3). The vapour equilibration technique (Scanlon et al., 2002) was used to measure the dry-end matric potential on sub-samples taken from each core. Soil water retention curves (SWRC) were modelled using the HypropFit (Schindler et al., 2010) (UMS, Munich, Germany) implementation of the Fredlund-Xing water retention model (Fredlund and Xing, 1994), using the measured soil water retention, dry bulk density, $K_{fs}$ (applied to cores from 0-0.05 m depth only) porosity, dry-end matric potential, volumetric moisture content and stoniness data.

Effective soil pore-size distribution was estimated using the method outlined by Blonquist et al. (2006). Hydraulic capacity was estimated using data from the SWRC (modelled in HypropFit) to derive the change in moisture over the change in hydraulic head ($d\theta_v/dh$). Hydraulic capacity was plotted as a function of pore radius. The scaled effective pore-size distribution associated with each tree species was then derived by taking the inverse relationship between pressure (h) from the water retention curve and log10 pore radius, resulting in a dimensionless, scaled, effective pore-size distribution. The distribution is displayed as a function of effective pore radius ƒ(r) proportional to the abundance of each pore-size within a given volume of soil.

To give context, *in situ* soil moisture was measured using ML3 ThetaProbe Soil Moisture Sensors (Delta-T Devices Ltd, Cambridge, UK) (n=9) in each plot at 10 cm depth. Particle-size distribution was ascertained using an air-dried sub-sample from soil used for the HYPROP analysis, repeatedly

quartered to mitigate selection bias (Lebron and Robinson, 2003) (Table 1). Particle-size distribution was determined from a 0.5-0.8 g subsample of sieved (<2 mm) soil using a LS13 320 laser diffraction particle-size analyser (Beckman Coulter Inc, Indianapolis, USA) (Table 1). Soil organic matter concentration was determined by loss-on-ignition (LOI) analysis of 10 g of sieved (<2 mm) soil (Ball, 1964) (Table 1). For quality assurance, two standard soil and two replicate samples were included for all LOI and particle size analyses.

### *2.5 Statistical analyses*

Two statistical models were used to analyse the datasets: (i) for the data collected from BangorDiverse (n=4), a two-factor ANOVA to test factors and interaction effects, with species and depth as factors, and root biomass, root morphological characteristics and $K_{fs}$ as dependant variables; (ii) for data collected at the pan-UK *F. excelsior* provenance trial sites (n=4), a two-factor ANOVA with soil classification and soil depth as factors and root biomass, root morphological characteristics and $K_{fs}$ as dependant variables. The Tukey Honest Significant Difference (HSD) post-hoc test was used to determine within-factor significance for both statistical models. Relationships between dependent variables were explored using ordinary linear regression. All data were tested for homogeneity of variance using Levene's test and normality using the Shapiro-Wilk's test. Root biomass, root morphological variables and $K_{fs}$ data were log transformed to satisfy normality. To visualise the relationships between variables, the dimensionality of the dataset was reduced from 44 parameters that included root morphological metrics (e.g., SRL, RAI, SRA, RLD) within three soil layers (0-0.1 m, 0.1-0.2 m and 0.2-0.3 m), $K_{fs}$ at the soil surface and soil porosity within two soil layers (0-0.05 m and 0.10-0.15 m) by conducting a principal component analysis (PCA). Stepwise multiple regression (forward and backwards) was then used to determine the parameter that best predicted $K_{fs}$. All statistical analyses were completed with SPSS v22.0 (IBM SPSS, Armonk, NY, USA) with $p < 0.05$ used as the limit for statistical significance. All figures were produced using SigmaPlot v13.0 (Systat Software, San Jose, CA, USA).

225 # 3. Results

226 ## *3.1 Tree species' effects*

227 ### 3.1.1 Hydraulic conductivity and root biomass

228 Mean surface $K_{fs}$ ranged from 3.47 ± 0.56 standard error cm $day^{-1}$ for *A. pseudoplatanus* to 7.91 ± 1.23
229 cm $day^{-1}$ for *F. excelsior*, although the difference between the species did not reach the threshold of
230 statistical significance ($p$=0.056) (Fig. 1a). However, a positive correlation (R253,254, = 0.64 (0-0.1 m
231 depth) and $R^2$ = 0.69 (0.1-0.2 m depth)) was observed between tree species' FRB and $K_{fs}$, with a high
232 degree of variation around mean $K_{fs}$ within some species (e.g. *Q. robur*).

233 Fine root biomass was affected by both species and soil depth ($p$<0.001), but no interaction effect was
234 evident (Table 2). *Fraxinus excelsior* was the species producing highest FRB at every soil depth (Table
235 3), with the largest difference in FRB between *F. excelsior* and the other species at a depth of 0-0.1
236 m($p$<0.001; Fig 1b). Fine root biomass of *F. excelsior* was between three-fold (*B. pendula*; $p$<0.001)
237 and six-fold (*C. sativa*; $p$<0.001) greater than the other species. Deeper in the soil where the
238 proportion of total *F. excelsior* FRB was much less (24%, 0.1-0.2 m; 17%, 0.2-0.3 m), *F. excelsior* FRB
239 was greater than *F. sylvatica* FRB only ($p$=0.05, 0.1-0.2 m; $p$<0.01, 0.2-0.3 m). The biomass:necromass
240 (B:N) ratio of *A. pseudoplatanus* (37.19) was significantly ($p$<0.05) greater than *A. glutinosa* (4.21) and
241 *C. sativa* (5.56) within the 0-0.1 m soil layer and was significantly greater for *A. pseudoplatanus* (103.9)
242 than *A. glutinosa* (3.27), *C. sativa* (1.05), *F. sylvatica* (6.60) and *Q. robur* (5.23) within the 0.1-0.2 m soil
243 layer ($p$<0.05).

244 Soil total porosity (0-0.05 m depth; Fig 1c) was similar between all species ($p$>0.05) at all soil depths.
245 Despite the aforementioned positive correlation between $K_{fs}$ and FRB, a similar relationship was not
246 observed between FRB and total porosity. There is some evidence of a positive linear relationship
247 between the mean $K_{fs}$ and FRB of each species, although it reached the $p$<0.05 threshold of
248 significance in the 0.1-0.2 m depth only. Fine root biomass explained 64, 69 and 25% of the variation
249 in $K_{fs}$ for the 0-0.1 m, 0.1-0.2 m and 0.2-0.3 m depths, respectively (Fig. 2a-c).

### 3.1.2 Soil water retention and pore-size distribution

Saturated soil water content was highest for *F. excelsior* (57%) and lowest for *F. sylvatica* (52%) in the 0-0.05 m soil layer (Fig. 3a). As soil water potential decreased, the soil water content under *F. excelsior* decreased rapidly, becoming comparable to the other species. Continued decreases in soil water potential caused *F. excelsior* to have the second lowest retention capacity. Conversely, *Q. robur* was ranked 5$^{th}$ in species' retention capacity at saturation but retained the highest percentage of soil water content at mid-range potentials (i.e., between -100 and -1000 cm). *Castanea sativa* had consistently low soil water content compared with the other species. Within the 0.10-0.15 m soil layer (Fig. 3b), *Q. robur* had the highest water content (57%) at saturation, whereas *F. excelsior* had the second lowest (50%), with *F. sylvatica* lowest (49%). All species had similar water content once pressure was applied (< -10 cm), apart from *C. sativa*, which again had consistently lower soil water content than other species.

Figures 3c and 3d show the scaled effective pore-size distribution. Soil developed under *F. excelsior* exhibited the greatest abundance (0.24) of macropores, followed by *B. pendula* (0.20), whilst the pore-size distributions of soil under *Q. robur* and *C. sylvatica* are skewed towards smaller pore sizes. By contrast, the proportion of macropores deeper in the soil (0.1-0.15 m) were similar amongst species, with the exception of *Q. robur* and *A. pseudoplatanus* (Fig 3d).

### 3.1.3 Root morphological traits

Tree species and separately soil depth affected all root traits (both $p<0.001$) except soil depth for SRA ($p>0.05$), but there were no species × depth interactions (Table 4). In the 0-1.0 m soil layer, *F. excelsior* had greater RLD (6.56 ± 0.65 cm cm$^{-3}$, $p<0.05$) and RAI (6.02 ± 0.86 m$^2$ m$^{-2}$, $p<0.01$) than all other species, more than 11 times greater than lowest ranked *C. sativa* (RLD 0.57 ± 0.07 cm cm$^{-3}$, RAI 0.51 ± 0.51 m$^2$ m$^{-2}$). Root tip density (RTD) was also greatest in *F. excelsior* (1275.01 ± 199.3 × 10$^2$m$^{-2}$), significantly more than *A. glutinosa (*242.89 ± 45.28 × 10$^2$ m$^{-2}$; $p<0.001$*)*, *C. sativa* (174.35 ± 17.17 × 10$^2$ m$^{-2}$; $p<0.001$) and *Q. robur* ($p<0.01$) (Table 5). The lowest RTD, associated with *C. sativa*, was more than seven-fold less than *F. excelsior. Fraxinus excelsior* had the greatest RLD, RAI and RTD in the 0.1-

0.2 m soil layer ($p$<0.01) and in the 0.2-0.3 m soil layer; RLD and RAI of *Fraxinus excelsior* (1.55 ± 0.47 cm $cm^{-3}$ RLD; 1.78 ± 0.57 $m^2$ $m^{-2}$ RAI) were three- to eight-fold and four- to seven-fold greater respectively than all other species ($p$<0.05) except *A. pseudoplatanus* ($p$>0.05; Table 5).

Ordination analysis was used to examine the relationship between tree root morphological traits and soil physical properties developed under the different tree species. The dimensionality of the data was reduced to three principal components (PC) that explained 95% of the variation. Principal component 1 explained 63%, PC2 18% and PC3 14% of the variation (Fig. 4). Tree species were tightly grouped together along the dominant PC1 with the exception of *F. excelsior*, which was strongly separated and associated most strongly with FRB, RAI, RTD, RLD and root projected surface area. Necromass was weakly separated from other root traits along PC2 and associated with *A. glutinosa* and *F. excelsior* (Fig 4a). Soil porosity in the 0-0.05 m depth and $K_{fs}$ were associated with each other along PC1 and weakly associated with *F. excelsior* and *A. glutinosa* along PC2 compared with the other five species, whereas, deeper in the soil (0.1-0.15 m), total porosity related more strongly to the other five species than *F. excelsior* and *A. glutinosa*. Fine root biomass and other morphological traits (i.e., root projected surface area, RAI, RTD and RLD) were all closely associated with each other along PC1, and with *F. excelsior*. Stepwise multiple regression analysis (forward and backward) showed that root necromass was the best single predictor of $K_{fs}$ ($R^2$ = 0.224; $p$<0.05) with all other variables excluded during the analysis.

### *3.2 Fraxinus excelsior across soil classifications*

Fine root biomass of *F. excelsior* differed significantly amongst soil depths and only between soil class where the fungal pathogen *Hymenoscyphus fraxineus*, which causes ash dieback disease on *F. excelsior* affected tree growth (i.e., Rendzic Leptosol). No interaction effect was evident between soil class and depth (Table 6). Fine root biomass was lowest in the Rendzic Leptosol through the whole profile (0-0.3 m), with a B:N ratio of 1.16, compared with the Haplic Luvisol (3.17), Dystric Fluvic Cambisol (6.62) and Dystric Gleysol (2.04) soils (SI 4). The relationship between FRB and hydraulic conductivity

301 previously observed across all tree species was reproduced when the relationship between *F. excelsior*
302 FRB and hydraulic conductivity was examined across the four soils; the $R^2$ was 0.49 for the two soil
303 layers 0-0.1 and 0.1-0.2 m and 0.43 for the 0.2-0.3 m layer.

304 Soil water retention curves were similar under *F. excelsior* across all four soil classifications in the
305 surface layer (Fig 5a). At saturation, the soil water content at 0.0-0.05 m depth did not vary
306 significantly and ranged between 61% and 57% for all soil classes. The shapes of the retention curves
307 were also similar throughout the range of water potentials. Conversely, SWRC from deeper in the soil
308 profile (0.1-0.15 m) differed substantially (Fig 5b). While the SWRC of the Dystric Gleysol from Devon
309 retained the same form as the surface soils, all other soils had decreased water retention at saturation
310 with depth. The two silty clay loam soils, Haplic Luvisol and Rendzic Leptosol, had the greatest change
311 in soil water content at saturation, both reducing from ~58% at the surface to ~48 and ~42%
312 respectively with depth. The silt loam, Haplic Luvisol, soil had a unimodal pore-size distribution, but
313 the other soils all had a bimodal distribution (Fig 5c&d). For all four soils macro- and meso-size pores
314 were clearly evident in the surface layer, but decreased with depth, particularly the mesopores, with
315 small pores becoming more prevalent with depth especially in the Dystric Gleysol and Haplic Luvisol
316 soils.

317 Compared with reference soils in the Rosetta database (Schaap et al., 2001), soils from the present
318 study retained a greater volume of water at saturation, regardless of soil classification (Fig. 6). The
319 modelled soil water retention, based on physical soil characteristics of agricultural soils, was 15-50%
320 less at saturation than those measured in the forested soils of the present study. Increasing soil water
321 potential (-cm) rapidly reduced the volumetric water content of measured SWRCs to become
322 comparable with the predicted reference soils by -100 cm.

## 323 4. Discussion

### 324 4.1 Tree root morphology and hydrology

This study showed that FRB production is tree species-specific, broadly agreeing with Chandler et al. (2018). Notably, *F. excelsior*, a ubiquitous species across much of Europe, establishes fine roots far more extensively, up to six-fold greater biomass, than the other common European broadleaved species assessed. Across species, total soil porosity remained consistent, but variation in FRB changed soil macroporosity and soil water retention. The results indicated that, although variation in species' FRB roughly mirrors that of $K_{fs}$, there was no relationship between FRB and total soil porosity. Soil under *F. excelsior* had the greatest water retention capacity at saturation (soil water potential = -1 cm), but the negligible variation between species indicated comparable total porosity. As soil water potential decreased the soil water content generated from soil collected under *F. excelsior* decreased rapidly, signifying the low bulk density and larger pore sizes (Radcliffe and Simunek, 2010) associated with *F. excelsior*.

Differences in pore-size distribution, rather than total porosity, linked to tree species-specific differences in fine root morphology are likely to be driving the relationship between tree species and hydraulic conductivity, but is moderated by fine root necromass. *Fraxinus excelsior* had the largest $K_{fs}$, root biomass and number of macropores, but the overall total porosity did not differ significantly from the soils under the other six tree species. The high FRB of *F. excelsior* might suggest adventitious root development and a greater RTD leading to the creation of macropores surrounding the root (Ghestem et al., 2011). However, it is apparent that FRB, projected root surface area and RTD are not as strongly related to porosity as are other root traits (Fig. 4). Despite the high FRB and hydraulic conductivity associated with *F. excelsior*, a correspondingly high RTD was not identified, suggesting that RLD, rather than RTD, is an important factor in the creation of macropore channels.

Despite nuanced relationships between live root morphological variables, macroporosity and $K_{fs}$, root necromass was the best predictor of $K_{fs}$ suggesting that root turnover has an important role in soil hydraulic function. Fine root longevity in trees is complex, ranging from days to years (Bengough, 2012) and is dependent on root diameter, root density, nitrogen concentration, colonisation of

mycorrhizal fungi and phenolic compound accumulation mediated by interaction with soil fauna (Eissenstat et al., 2000). During root development, exuded organic compounds contribute to the stability of the root channel, but following root death dehydration initially occurs, allowing gradual decomposition that creates progressively larger channels within the soil matrix available for preferential flow, and subsequently sub-surface sediment transfer causes channels to collapse or fill over time (Bengough, 2012; Ghestem et al., 2011). Variation in root turnover rates should have a large influence on the size and longevity of root-derived macropores (Wang et al., 2020).

Tree root morphological traits in this study better explained $K_{fs}$ variations near the soil surface (0-0.2 m) than deeper in the soil (0.2-0.3 m depth). Root length density was greatest near the soil surface facilitating connectivity of root-induced macropores and greater opportunity for infiltration. A similar strong relationship between macroporosity near the soil surface and preferential flow in three tree species (*Styphnolobium japonicum* (L.) Schott*, Platycladus orientalis* (L.) Franco, and *Quercus dentata* Thunb.), which diminished with depth, has also been reported (Zhang et al., 2015). A comparison with pedotransfer functions, largely used for agricultural soils, indicated that, by excluding sub-surface flow through macropores, hydraulic functions quickly converge with those predicted by the pedotransfer functions for the given soil texture in the 0-0.1 m soil layer. However, deeper in the profile (0.1-0.3 m) where the density of fine roots is lower, soil texture had a greater influence on soil hydraulic conductivity. Results of the present study, combined with the apparent lack of accountability for macropores generated by trees in pedotransfer functions, suggests that improvement could be made to the parameterisation of hydrological models based on the below-ground characteristics of vegetation.

### *4.2 Soil classification and hydrology*

Our study explored whether variation due to soil textural properties would temper the influence of afforestation with a single tree species (*F. excelsior*) on water retention capacity. Data from the forested plots were compared to agricultural soils with the same textural properties (loam, silty clay

loam and clay loam) in the Rosetta database to obtain comparable values of hydraulic response. Modification of soil structure by the presence of trees enabled greater water retention capacity at saturation (Fig. 6). As water potential increased, which effectively excludes the influence of macropores, the forest SWRCs migrate closer to the Rosetta predictions. Therefore, landcover, specifically the presence of trees, appears to mediate the influence of soil textural properties on hydraulic response, regardless of soil classification, although within landcovers impacts, such as tillage, may regulate the response.

Using *F. excelsior* as an example, this study showed that soil texture, a considerable influence on ambient soil moisture, does not influence fine root growth near the soil surface. Furthermore, in the 0-0.1 m depth, fine tree roots modified pore-size distribution, negating the effect of soil class on hydrological function. At 0-0.1 m depth, where 50-58% of total FRB of *F. excelsior* was present, little variation in soil water retention was observed between sites differing in soil classification. Deeper in the soil, soil water retention was more divergent amongst sites as the influence of fine roots decreased and soil class started to dominate the hydraulic response. Hydraulic conductivity, therefore, is influenced by the combination of root morphology and soil classification, which varied with depth. Indeed, within-species variation in root morphology and rooting extent throughout the soil profile has been shown to be contingent on ambient hydrological soil conditions, oxygen availability and access to groundwater resources (Feng et al., 2017).

During very dry conditions, such as those recently preceding the study period (mean volumetric soil water content of 16%), soil class had a nuanced effect on rooting morphology and macroporosity. The sandy silt loam and clay loam textures of the Dystric Fluvic Cambisol and Dystric Gleysol exhibited similar pore-size distributions. By contrast, the silty clay texture of the Haplic Luvisol was associated with a lower FRB. There was a lack of organic matter, or limestone, in the Haplic Luvisol that could disaggregate the clay compared with the other clay-containing soils (i.e., Dystric Gleysol and Rendzic Leptosol). The high clay content resulted in a substantially hardened soil that reduced plasticity and

was likely to be related to the observed lower abundance of macropores. Root dieback, however, caused by tree disease may have a greater, though time limited, impact on soil hydraulic function than soil classification. Root dieback is positively associated with crown reduction due to infection from *Hymenoscyphus fraxineus* (Bakys et al., 2011). Where *H. fraxineus* was observed at a moderate - advanced stage (assessment methods described in SI) (i.e., Hampshire; Rendzic Leptosol), necromass accounted for half of the total fine root mass (B:N = 0.98) in the 0-0.1 m depth, substantially more than in the other clay-dominant soils (Haplic Luvisol, 2.49; Dystric Gleysol, 2.05). Once necromass has fully decomposed, the residual root channels will be vulnerable to collapse, potentially reducing hydraulic conductivity in the longer-term.

### *4.3 Implications for land managers*

*Fraxinus excelsior* had the greatest potential to improve surface water infiltration regardless of soil class. A ubiquitous species in much of Europe, *F. excelsior* is likely to have a disproportionately larger influence on landscape hydraulic function than the other tree species assessed here due to its root morphology and influence on macroporosity.. Therefore, loss of *F. excelsior* in the landscape due to the fungal pathogen *H. fraxineus* could have serious implications for local soil hydrological function throughout Europe. Consideration of hydraulic function should be a major component in the selection of alternative tree species to replace *F. excelsior*, and tree species' root morphological traits and influence on soil hydrology should be used as a criterion to select tree species in the future to maximise the potential benefits of establishing new woodlands. However, whilst results of the present study showed that tree species-specific root morphological traits have a role in altering soil hydraulic function at the plot scale, the complex interactions that influence catchment hydrology (e.g., field boundaries, land use and drainage) suggest that caution should be exercised before extrapolating such plot-scale results to the landscape scale.

## 5. Conclusion

Species-specific variation in fine root morphological characteristics of seven common European broadleaved tree species were shown to alter soil macroporosity and hydraulic function. Fine root length density and necromass were correlated with an increased abundance of macropores within the soil, facilitating greater hydraulic conductivity, despite little change in total porosity. Notably, *F. excelsior* had up to a six-fold greater FRB than the other tree species studied, however RLD rather than FRB was shown to be the strongest driver of the observed changes in macroporosity.

Soil water retention curves and porosity data indicated that tree roots influence soil structural characteristics in the 0-0.1 m layer of the soil, where more than 50% of the FRB was present, maximising macroporosity regardless of soil texture. Species with the greatest RLD exhibited correspondingly greater macropore abundance and higher hydraulic conductivity when soils were at or close to saturation.

The species-specific influence of trees on hydraulic function and the associated impact of tree diseases, such as the fungal pathogen *Hymenoscyphus fraxineus* which causes ash dieback disease on *F. excelsior*, suggests that changes to the composition of tree species present in the landscape could have implications for hydrological hydraulic regulation. Further work is necessary to determine if hydrological models can be improved by the incorporation of below-ground tree trait data.

## Acknowledgements

All authors acknowledge the financial support provided by the Welsh Government and Higher Education Funding Council for Wales through the Sêr Cymru National Research Network for Low Carbon, Energy and Environment. We thank Forest Research for permitting access to the ash provenance research network field sites for collection of soil cores and hydrological data. We acknowledge access given by Rothamsted Research at North Wyke Farm to *F. excelsior* stands.

## References


Ahmed, I.U., Smith, A.R., Jones, D.L., Godbold, D.L., 2016. Tree species identity influences the vertical distribution of labile and recalcitrant carbon in a temperate deciduous forest soil. For. Ecol. Manage. 359, 352–360. https://doi.org/10.1016/j.foreco.2015.07.018

Avery, B.W., 1980. Soil Classification for England and Wales (Higher Categories). Soil Survey Technical Monograph No. 14. Harpenden.

Bakys, R., Vasiliauskas, A., Ihrmark, K., Stenlid, J., Menkis, A., Vasaitis, R., 2011. Root rot, associated fungi and their impact on health condition of declining *Fraxinus excelsior* stands in Lithuania. Scand. J. F. Res. 26, 128-135. https://doi.org/10.1080/02827581.2010.536569

Ball, D.F., 1964. Loss-on-Ignition as an estimate of organic matter and organic carbon in non-calcareous Soils. J. Soil Sci. 15, 84–92. https://doi.org/10.1111/j.1365-2389.1964.tb00247.x

Bargues Tobella, A., Reese, H., Almaw, A., Bayala, J., Malmer, A., Laudon, H., Ilstedt, U., 2014. The effect of trees on preferential flow and soil infiltrability in an agroforestry parkland in semiarid Burkina Faso. Water Resour. Res. 50, 3342–3354. https://doi.org/10.1002/2013WR015197

Bathurst, J., Birkinshaw, S., Johnson, H., Kenny, A., Napier, A., Raven, S., Robinson, J., Stroud, R., 2018. Runoff, flood peaks and proportional response in a combined nested and paired forest plantation/peat grassland catchment. J. Hydrol. 564, 916–927. https://doi.org/10.1016/j.jhydrol.2018.07.039

Bengough, A.G., 2012. Water dynamics of the root zone: rhizosphere biophysics and its control on soil hydrology. Vadose Zone Journal 11, vzj2011.0111. https://doi.org/10.2136/vzj2011.0111

Blonquist, J.M., Jones, S.B., Lebron, I., Robinson, D.A., 2006. Microstructural and phase configurational effects determining water content: dielectric relationships of aggregated porous media. Water Resour. Res. 42, 1–13. https://doi.org/10.1029/2005WR004418

Bodner, G., Leitner, D., Kaul, H., 2014. Coarse and fine root plants affect pore size distributions differently. Plant Soil 380, 133–151. https://doi.org/10.1007/s11104-014-2079-8

Carrick, J., Bin Abdul Rahim, M.S.A., Adjei, C., Habib, H., Ashraa Kalee, H.H.H., Banks, S.J., Bolam, F.C., Campos Luna, I.M., Clark, B., Cowton, J., Nongando Domingos, I.F., Golicha, D.D., Gupta, G., Grainger, M., Hasanaliyeva, G., Hodgson, D.J., Lopez-Capel, E., Magistrali, A.J., Merrell, I.G., Oikeh, I., Othman, M.S., Ranathunga Mudiyanselage, T.K.R., Samuel, C.W.C., Sufar, E.K.H., Watson, P.A., Zakaria, N.N.A.B., Stewart, G., 2019. Is planting trees the solution to reducing flood risks? J. Flood Risk Manag. 12, 1–10. https://doi.org/10.1111/jfr3.12484

476 Chandler, K.R., Chappell, N.A., 2008. Influence of individual oak (*Quercus robur*) trees on saturated
477 hydraulic conductivity. For. Ecol. Manage. 256, 1222–1229.
478 https://doi.org/10.1016/j.foreco.2008.06.033

479 Chandler, K.R., Stevens, C.J., Binley, A., Keith, A.M., 2018. Influence of tree species and forest land use
480 on soil hydraulic conductivity and implications for surface runoff generation. Geoderma 310, 120–127.
481 https://doi.org/10.1016/j.geoderma.2017.08.011

482 Creed, I.F., van Noordwijk, M. (Eds.), 2018. Forest and water on a changing planet: vulnerability,
483 adaptation and governance opportunities. A global assessment report. IUFRO World Series volume
484 38, Vienna, Austria.

485 Cundall, E.P., Cahalan, C.M., Connolly, T., 2003. Early results of ash (*Fraxinus excelsior* L.) provenance
486 trials at sites in England and Wales. Forestry 76, 385-400. https://doi.org/10.1093/forestry/76.4.385

487 Dadson, S.J., Hall, J.W., Murgatroyd, A., Acreman, M., Bates, P., Beven, K., Heathwaite, L., Holden, J.,
488 Holman, I.P., Lane, S.N., O'Connell, E., Penning-Rowsell, E., Reynard, N., Sear, D., Thorne, C., Wilby, R.,
489 2017. A restatement of the natural science evidence concerning catchment-based "natural" flood
490 management in the UK. Proc. R. Soc. A Math. Phys. Eng. Sci. 473.
491 https://doi.org/10.1098/rspa.2016.0706

492 Dixon, S.J., Sear, D.A., Odoni, N.A., Sykes, T., Lane, S.N., 2016. The effects of river restoration on
493 catchment scale flood risk and flood hydrology. Earth Surf. Process. Landforms, 41 997-1008.
494 https://doi.org/10.1002/esp.3919

495 Eissenstat, D.M., Yanai R.D. 1997 The ecology of root lifespan. Adv Ecol Res 27:1–60.
496 https://doi.org/10.1016/S0065-2504(08)60005-7

497 Eissenstat, D.M., Wells, C.E., Yanai, R.D., Whitbeck, J.L., 2000. Building roots in a changing
498 environment: implications for root longevity. New Phytol. 147, 33–42.
499 https://doi.org/10.1046/j.1469-8137.2000.00686.x

500 Fan, Y., Miguez-Macho, G., Jobbágy, E.G., Jackson, R.B., Otero-Casal, C., 2017. Hydrologic regulation
501 of plant rooting depth. Proc. Natl. Acad. Sci. U.S.A. 114, 10572–10577.
502 https://doi.org/10.1073/pnas.1712381114

503 Fischer, C., Tischer, J., Roscher, C., Eisenhauer, N., Ravenek, J., Gleixner, G., Attinger, S., Jensen, B., de
504 Kroon, H., Mommer, L., Scheu, S., Hildebrandt, A., 2015. Plant species diversity affects infiltration
505 capacity in an experimental grassland through changes in soil properties. Plant Soil 397, 1–16.
506 https://doi.org/10.1007/s11104-014-2373-5

507 Fredlund, D.G., Xing, A., 1994. Equations for the soil-water characteristic curve. Can. Geotech. J. 31,
508 521–532. https://doi.org/10.1139/t94-061

509 Geris, J., Tetzlaff, D., McDonnell, J., Soulsby, C., 2015. The relative role of soil type and tree cover on
510 water storage and transmission in northern headwater catchments. Hydrol. Process. 29, 1844-1860.
511 https://doi.org/10.1002/hyp.10289

512 Gerke, K.M., Sidle, R.C., Mallants, D., 2015. Preferential flow mechanisms identified from staining
513 experiments in forested hillslopes. Hydrol. Process. 29, 4562-4578.
514 https://doi.org/10.1002/hyp.10468

515 Ghestem, M., Sidle, R.C., Stokes, A., 2011. The influence of plant root systems on subsurface flow:
516 implications for slope stability. Bioscience 61, 869–879. https://doi.org/10.1525/bio.2011.61.11.6

517 Gunina, A., Smith, A.R., Kuzyakov, Y., Jones, D.L., 2017. Microbial uptake and utilization of low
518 molecular weight organic substrates in soil depend on carbon oxidation state. Biogeochemistry 133,
519 89–100. https://doi.org/10.1007/s10533-017-0313-1

520 IPCC, 2014. Climate change 2014: Synthesis Report. Contribution of Working Groups I, II and III to the
521 Fifth Assessment Report of the Intergovernmental Panel on Climate Change. IPCC, Geneva,
522 Switzerland.

523 IUSS Working Group WRB, 2015. World reference base for soil resources 2014, update 2015
524 International soil classification system for naming soils and creating legends for soil maps, World Soil
525 Resources Reports No. 106. FAO, Rome.

526 Jarvis, N., Koestel, J., Messing, I., Moeys, J., Lindahl, A., 2013. Influence of soil, land use and climatic
527 factors on the hydraulic conductivity of soil. Hydrol. Earth Syst. Sci. Discuss. 17, 5185–5195.
528 https://doi.org/10.5194/hess-17-5185-2013

529 Johnson-Maynard, J.L., Graham, R.C., Wu, L., Shouse, P.J., 2002. Modification of soil structural and
530 hydraulic properties after 50 years of imposed chaparral and pine vegetation. Geoderma 110, 227–
531 240. https://doi.org/https://doi.org/10.1016/S0016-7061(02)00232-X

532 Kosugi, K., Hopmans, J.W., Dane, J.H., 2002. Parametric models, in: Dane, J.H., Topp, G.C. (Eds.),
533 Methods of Soil Analysis: Part 4 Physical Methods, 5.4. Soil Science Society of America, Inc., Madison,
534 Wisconsin, pp. 739-757.

535 Lane, S.N., 2017. Natural flood management. WIREs Water 4, e1211.
536 https://doi.org/10.1002/wat2.1211

537 Lebron, I., Robinson, D.A., 2003. Particle size segregation during hand packing of coarse granular
538 materials and impacts on local pore-scale structure. Vadose Zone 2, 330–337.
539 https://doi.org/10.2113/2.3.330

540 Lohmus, K., Oja, T., Lasn, R., 1989. Specific root area: a soil characteristic 249, 245–249.
541 https://doi.org/10.1007/BF02370415

542 Luo, Z., Niu, J., Zhang, L., Chen, X., Zhang, W., Xie, B., Du, J., Zhu, Z., Wu, S., Li, X., 2019. Roots-enhanced
543 preferential flows in deciduous and coniferous forest soils revealed by dual-tracer experiments. J.
544 Environ. Qual. 48, 136–146. https://doi.org/10.2134/jeq2018.03.0091

545 Marshall, M.R., Francis, O.J., Frogbrook, Z.L., Jackson, B.M., McIntyre, N., Reynolds, B., Solloway, I.,
546 Wheater, H.S., Chell, J., 2009. The impact of upland land management on flooding: results from an
547 improved pasture hillslope. Hydrol. Process. 23, 464–475. https://doi.org/10.1002/hyp.7157

548 Marshall, M.R., Ballard, C.E., Frogbrook, Z.., Solloway, I., McIntyre, N., Reynolds, B., Wheater, H.S.,
549 2013. The impact of rural land management changes on soil hydraulic properties and runoff processes:
550 results from experimental plots in upland UK. Hydrol. Process. 28, 2617–2629.
551 https://doi.org/10.1002/hyp.9826

552 Mcintyre, N., Thorne, C., 2013. Land use management effects on flood flows and sediments - guidance
553 on prediction. CIRIA, London.
554 https://www.ciria.org/ItemDetail?iProductCode=C719F&Category=FREEPUBS (accessed 23 March
555 2017).

556 Meter Group Inc, 2018. Mini Disk Infiltrometer. Pullman, WA, USA.
557 https://www.metergroup.com/environment/products/mini-disk-infiltrometer/ (accessed 15
558 September 2016).

559 Mrak, T., Gricar, J., 2016. Atlas of Woody Plant Roots: morphology and anatomy with special emphasis
560 on fine roots. Slovenian Forestry Institute, The Silva Slovenica Publishing Centre.

561 Ostonen, I., Püttsepp, Ü., Biel, C., Alberton, O., Bakker, M.R., Lõhmus, K., Metcalfe, D., Olsthoorn,
562 A.F.M., Pronk, A., Vanguelova, E., Weih, M., Brunner, I., 2007. Specific root length as an indicator of
563 environmental change, Plant Biosyst., 143:3 426-442 3504.
564 https://doi.org/10.1080/11263500701626069

565 Pliura, A., Bakys, V., Suchockas, D., Marciulyniene, D., Gustiene, A., Verbyla, V., Lygis, V., 2011. Ash
566 dieback in Lithuania: disease history, research on impact and genetic variation in disease resistance,
567 tree breeding and options for forest management, in: Vasaitis, R., Enderle, R. (Eds.), Dieback of

568 European Ash (*Fraxinus* Spp.) Consequences and Guidelines for Sustainable Management. COST
569 (European Cooperation in Science and Technology), Uppsala, Sweden.

570 Radcliffe, D.E., Simunek, J., 2010. Soil Water Content and Potential, in: Radcliffe, D.., Simunek, J. (Eds.),
571 Soil Physics with Hydrus: Modeling and Applications. Taylor & Francis, Boca Raton, Florida.

572 Scanlon, B.R., Andraski, B.J., Bilskie, J., 2002. Water potential: miscellaneous methods for measuring
573 matric or water potential., in: Dane, J.H., Topp, G.C. (Eds.), Methods of Soil Analysis. Part 4 - Physical
574 Methods. Soil Science Society of America, Madison, WI, pp. 643–670.
575 https://doi.org/10.2136/sssabookser5.4.c23

576 Schaap, M.G., Leij, F.J., Genuchten, M.T. Van, 2001. ROSETTA : a computer program for estimating soil
577 hydraulic parameters with hierarchical pedotransfer functions. J. Hydrol. 251, 163–176.
578 https://doi.org/10.1016/S0022-1694(01)00466-8

579 Schindler, U., Durner, W., von Unold, G., Mueller, L., Wieland, R., 2010. The evaporation method:
580 Extending the measurement range of soil hydraulic properties using the air-entry pressure of the
581 ceramic cup. J. Plant Nutr. Soil Sci. 173, 563–572. https://doi.org/10.1002/jpln.200900201

582 Sinacore, K., Hall, J.S., Potvin, C., Royo, A.A., Ducey, M.J., Ashton, M.S., 2017. Unearthing the hidden
583 world of roots: root biomass and architecture differ among species within the same guild. PLoS One
584 12, e0185934. https://doi.org/10.1371/journal.pone.0185934

585 Smith, A.R., Lukac, M., Bambrick, M., Miglietta, F., Godbold, D.L., 2013. Tree species diversity interacts
586 with elevated $CO_2$ to induce a greater root system response. Glob. Chang. Biol. 19, 217–228.
587 https://doi.org/10.1111/gcb.12039

588 Spurgeon, D.J., Keith, A.M., Schmidt, O., Lammertsma, D.R., Faber, J.H., 2013. Land-use and land-
589 management change: relationships with earthworm and fungi communities and soil structural
590 properties. BMC Ecology 13, 46. https://doi.org/10.1186/1472-6785-13-46

591 Stratford, C., Miller, J., House, A., Old, G., Acreman, M., Duenas-Lopez, M., Nisbet, T., Newman, J.,
592 Burgess-Gamble, L., Chappell, N., Clarke, N., Leeson, L., Monbiot, G., Paterson, J., Robinson, M.,
593 Rogers, M., Tickner, D., 2017. Do trees in UK-relevant river catchments influence fluvial flood peaks?
594 (No. CEH Project no. NEC06063). Wallingford, UK.
595 http://nora.nerc.ac.uk/id/eprint/517804/7/N517804CR.pdf (accessed 23 January, 2021).

596 Sun, D., Yang, H., Guan, D., Yang, M., Wu, J., Yuan, F., Jin, C., Wang, A., Zhang, Y., 2018. The effects of
597 land use change on soil infiltration capacity in China: a meta-analysis. Sci. Total Environ. 626, 1394–
598 1401. https://doi.org/10.1016/j.scitotenv.2018.01.104

599 Thompson, S.E., Harman, C.J., Heine, P., Katul, G.G., 2010. Vegetation - infiltration relationships across
600 climatic and soil type gradients. J. Geophys. Res. 115, G02023.
601 https://doi.org/https://doi.org/10.1029/2009JG001134

602 Wang, N., Wang, C., Quan, X., 2020. Variations in fine root dynamics and turnover rates in five forest
603 types in northeastern China. J. For. Res. 31, 871–884. https://doi.org/10.1007/s11676-019-01065-x

604 Wolton, R., Pollard, K., Goodwin, A., Norton, L., 2014. Regulatory services delivered by hedges : the
605 evidence base. Report of Defra project LM0106.
606 http://sciencesearch.defra.gov.uk/Document.aspx?Document=12096_LM0106_final_report.pdf
607 (accessed 1 March 2017)

608 World Reference Base (WRB) for soil resources, 2006. World Soil Resources Reports No. 103. Rome.
609 http://www.fao.org/soils-portal/soil-survey/soil-classification/world-reference-base/en

610 Zhang, R., 1997. Determination of soil sorptivity and hydraulic conductivity from the disk infiltrometer.
611 Soil Sci. Soc. Am. 61, 1024–1030. https://doi.org/DOI: 10.2136/sssaj1997.03615995006100040005x

612 Zhang, Y.H., Niu, J.Z., Yu, X.X., Zhu, W.L., Du, X.Q., 2015. Effects of fine root length density and root
613 biomass on soil preferential flow in forest ecosystems. For. Syst. 24, 1–11.
614 http://dx.doi.org/10.5424/fs/2015241-06048.

615 **Tables**

**Table 1.** Location of *Fraxinus excelsior* provenance trial experimental plots by World Reference Base (WRB) soil classification (WRB for soil resources, 2006), UK county, mean particle size distribution of the mineral soil to 0.015 m soil depth and soil texture based on measured soil particle size distribution (Soil Classification for England and Wales) (Avery, 1980).

| WRB classification soil group | Site (UK county) | Latitude Longitude | Mean soil particle size distribution (%) | | | Soil texture | Mean soil organic matter content (%) |
|---|---|---|---|---|---|---|---|
| | | | Sand | Silt | Clay | | |
| Dystric Fluvic Cambisol | Gwynedd | 53° 14′ 19.38″ N 4° 01′ 05.91″ W | 40 | 44 | 16 | Sandy silt loam | 6.4 |
| Haplic Luvisol | Gloucestershire | 51° 54′ 24.93″ N 2° 18′ 39.68″ W | 20 | 59 | 21 | Silty clay loam | 6.5 |
| Rendzic Leptosol | Hampshire | 51° 12′ 02.02″ N 1° 31′ 39.48″ W | 16 | 57 | 26 | Silty clay loam – limestone rich | 7.0 |
| Dystric Gleysol | Devon | 50° 46′ 12.14″ N 3° 54′ 08.79″ W | 25 | 51 | 23 | Clay loam | 11.5 |

Table 2. Main effects of seven tree species' *(Alnus glutinosa, Fraxinus excelsior, Fagus sylvatica, Betula pendula, Castanea sativa, Quercus robur* and *Acer pseudoplatanus)* fine root biomass in three soil depths (0-0.1, 0.1-0.2, 0.2-0.3 m).

| Factor | df | F | *p*-value |
|---|---|---|---|
| Depth | 2 | 16.156 | <0.001 |
| Species | 6 | 11.677 | <0.001 |
| Depth*Species | 12 | 0.831 | 0.618 |

623

624 Table 3. Mean fine root biomass and rank order of seven tree species *(Alnus glutinosa, Fraxinus*
625 *excelsior, Fagus sylvatica, Betula pendula, Castanea sativa, Quercus robur* and *Acer pseudoplatanus)*
626 at 0.1 m depth intervals and for the whole sampled profile (0-0.3 m). Mean fine root biomass at each
627 depth is given as a proportion of the whole profile (0-0.3 m) fine root biomass (%), B:N describes the
628 biomass:necromass ratio. SE = ±1 standard error. Superscript letters denote Tukey post hoc
629 comparison ($p < 0.05$) between species within each soil depth.

| | Fine root biomass (kg $m^{-2}$) | | Rank order | Proportion of total fine root biomass (%) | Necromass (kg $m^{-2}$) | | B:N ratio | |
|---|---|---|---|---|---|---|---|---|
| **0–0.1 m** | Mean | SE | | | Mean | SE | Mean | SE |
| *Alnus glutinosa* | $0.84^{b}$ | ± 0.15 | 4 | 60.31 | 0.25 | ± 0.05 | $4.21^{b}$ | ± 1.53 |
| *Fraxinus excelsior* | $3.05^{a}$ | ± 0.40 | 1 | 59.01 | 0.36 | ± 0.14 | $12.17^{ab}$ | ± 3.69 |
| *Fagus sylvatica* | $0.55^{b}$ | ± 0.12 | 6 | 51.36 | 0.03 | ± 0.01 | $16.85^{ab}$ | ± 3.69 |
| *Betula pendula* | $1.12^{b}$ | ± 0.13 | 2 | 48.71 | 0.14 | ± 0.05 | $10.08^{ab}$ | ± 2.13 |
| *Castanea sativa* | $0.45^{b}$ | ± 0.09 | 7 | 36.91 | 0.07 | ± 0.04 | $5.56^{b}$ | ± 2.81 |
| *Quercus robur* | $0.62^{b}$ | ± 0.29 | 5 | 49.10 | 0.12 | ± 0.07 | $7.30^{ab}$ | ± 2.51 |
| *Acer pseudplatanus* | $0.87^{b}$ | ± 0.28 | 3 | 42.88 | 0.08 | ± 0.06 | $37.19^{a}$ | ± 16.73 |
| **0.1–0.2 m** | | | | | | | | |
| *Alnus glutinosa* | 0.26 | ± 0.07 | 7 | 19.04 | 0.15 | ± 0.05 | $3.27^{b}$ | ± 1.92 |
| *Fraxinus excelsior* | 1.22 | ± 0.31 | 1 | 23.56 | 0.11 | ± 0.03 | $15.16^{ab}$ | ± 4.73 |
| *Fagus sylvatica* | 0.35 | ± 0.11 | 6 | 32.45 | 0.05 | ± 0.02 | $6.60^{b}$ | ± 3.76 |
| *Betula pendula* | 0.74 | ± 0.08 | 2 | 31.99 | 0.06 | ± 0.02 | $14.05^{ab}$ | ± 2.42 |
| *Castanea sativa* | 0.41 | ± 0.10 | 4 | 33.62 | 0.17 | ± 0.06 | $1.05^{b}$ | ± 0.40 |
| *Quercus robur* | 0.38 | ± 0.10 | 5 | 30.29 | 0.08 | ± 0.03 | $5.23^{b}$ | ± 1.23 |
| *Acer pseudoplatanus* | 0.52 | ± 0.11 | 3 | 25.51 | 0.03 | ± 0.02 | $103.9^{a}$ | ± 54.77 |
| **0.2–0.3 m** | | | | | | | | |
| *Alnus glutinosa* | $0.29^{ab}$ | ± 0.05 | 5 | 20.66 | 0.11 | ± 0.03 | 3.82 | ± 1.95 |
| *Fraxinus excelsior* | $0.90^{a}$ | ± 0.32 | 1 | 17.43 | 0.11 | ± 0.06 | 10.67 | ± 2.73 |
| *Fagus sylvatica* | $0.17^{b}$ | ± 0.04 | 7 | 16.18 | 0.02 | ± 0.00 | 8.96 | ± 2.80 |
| *Betula pendula* | $0.44^{ab}$ | ± 0.06 | 3 | 19.30 | 0.08 | ± 0.01 | 6.95 | ± 1.86 |
| *Castanea sativa* | $0.36^{ab}$ | ± 0.13 | 4 | 29.47 | 0.05 | ± 0.02 | 2.57 | ± 1.05 |

| | | | | | | | | |
|---|---|---|---|---|---|---|---|---|
| *Quercus robur* | 0.26[ab] | ± 0.04 | 6 | 20.61 | 0.09 | ± 0.03 | 3.78 | ± 1.05 |
| *Acer pseudoplatanus* | 0.64[a] | ± 0.19 | 2 | 31.61 | 0.12 | ± 0.05 | 12.61 | ± 6.33 |
| **0–0.3 m** | | | | | | | | |
| *Alnus glutinosa* | 1.39[b] | ± 0.26 | 4 | N/A | 0.51 | ± 0.11 | 3.43 | ± 1.20 |
| *Fraxinus excelsior* | 5.16[a] | ± 0.71 | 1 | N/A | 0.58 | ± 0.17 | 12.01 | ± 3.83 |
| *Fagus sylvatica* | 1.07[b] | ± 0.26 | 7 | N/A | 0.11 | ± 0.03 | 10.68 | ± 2.84 |
| *Betula pendula* | 2.30[ab] | ± 0.12 | 2 | N/A | 0.27 | ± 0.05 | 9.30 | ± 1.78 |
| *Castanea sativa* | 1.21[b] | ± 0.24 | 6 | N/A | 0.29 | ± 0.10 | 1.97 | ± 0.73 |
| *Quercus robur* | 1.26[b] | ± 0.34 | 5 | N/A | 0.30 | ± 0.09 | 4.57 | ± 0.81 |
| *Acer pseudoplatanus* | 2.04[ab] | ± 0.56 | 3 | N/A | 0.23 | ± 0.07 | 14.82 | ± 6.65 |

Table 4 Between-subject effects of species and depth on fine root traits including specific root length (m $g^{-1}$), root area index ($m^2$ $m^{-2}$), specific root surface area ($m^2$ $kg^{-1}$), root length density (cm $cm^{-3}$) and root tip density (× $10^3$ $m^{-2}$).

| | | df | F-statistic | *p* |
|---|---|---|---|---|
| Species | Specific root length (m $g^{-1}$) | 6 | 21.825 | <0.001 |
| | Root area index ($m^2$ $m^{-2}$) | 6 | 22.757 | <0.001 |
| | Specific root surface area ($m^2$ $kg^{-1}$) | 6 | 19.549 | <0.001 |
| | Root length density (cm $cm^{-3}$) | 6 | 29.519 | <0.001 |
| | Root tip density (x $10^2$ $m^{-2}$) | 6 | 25.816 | <0.001 |
| Depth | Specific root length (m $g^{-1}$) | 2 | 76.572 | <0.001 |
| | Root area index ($m^2$ $m^{-2}$) | 2 | 22.994 | <0.001 |
| | Specific root surface area ($m^2$ $kg^{-1}$) | 2 | 0.591 | 0.557 |
| | Root length density (cm $cm^{-3}$) | 2 | 39.089 | <0.001 |
| | Root tip density (x $10^2$ $m^{-2}$) | 2 | 57.046 | <0.001 |
| Species×Depth | Specific root length (m $g^{-1}$) | 12 | 0.395 | 0.961 |
| | Root area index ($m^2$ $m^{-2}$) | 12 | 0.826 | 0.623 |
| | Specific root surface area ($m^2$ $kg^{-1}$) | 12 | 0.392 | 0.962 |
| | Root length density (cm $cm^{-3}$) | 12 | 0.852 | 0.598 |
| | Root tip density (x $10^2$ $m^{-2}$) | 12 | 1.108 | 0.370 |

**Table 5.** Fine root metrics (specific root length (m $g^{-1}$), root area index ($m^2$ $m^{-2}$), specific root surface area ($m^2$ $kg^{-1}$), root length density (cm $cm^{-3}$) and root tip density (x $10^2$ $m^{-2}$) of seven tree species (*Alnus glutinosa, Fraxinus excelsior, Fagus sylvatica, Betula pendula, Castanea sativa, Quercus robur* and *Acer*

638 *pseudoplatanus*) at three soil depths (0-0.1, 0.1-0.2, 0.2-0.3 m). SE = ±1 standard error. Superscript letters denote Tukey post hoc comparisons ($p < 0.05$) of

639 root traits within each soil depth.

| **Root trait** | **Depth** | ***Alnus glutinosa*** | | | ***Fraxinus excelsior*** | | | ***Fagus sylvatica*** | | | ***Betula pendula*** | | | ***Castanea sativa*** | | | ***Quercus robur*** | | | ***Acer pseudoplatanus*** | | |
|---|---|---|---|---|---|---|---|---|---|---|---|---|---|---|---|---|---|---|---|---|---|---|
| Specific root length (m $g^{-1}$) | 0-0.1 | $8.27^{b}$ | ± | 1.94 | $22.23^{a}$ | ± | 3.62 | $26.38^{a}$ | ± | 3.22 | $14.88^{ab}$ | ± | 1.58 | $13.43^{ab}$ | ± | 1.22 | $20.20^{a}$ | ± | 3.04 | $22.43^{a}$ | ± | 3.57 |
| | 0.1-0.2 | $4.13^{c}$ | ± | 0.41 | $10.09^{ab}$ | ± | 0.45 | $13.45^{a}$ | ± | 3.85 | $6.36^{abc}$ | ± | 0.29 | $5.79^{bc}$ | ± | 0.83 | $9.88^{ab}$ | ± | 2.50 | $9.42^{ab}$ | ± | 0.38 |
| | 0.2-0.3 | $3.37^{c}$ | ± | 0.45 | $8.98^{ab}$ | ± | 0.73 | $11.78^{a}$ | ± | 1.66 | $5.35^{bc}$ | ± | 0.57 | $5.53^{bc}$ | ± | 0.95 | $9.31^{ab}$ | ± | 1.06 | $6.52^{ab}$ | ± | 1.12 |
| Root area index ($m^2$ $m^{-2}$) | 0-0.1 | $0.88^{b}$ | ± | 0.27 | $6.02^{a}$ | ± | 0.86 | $0.96^{b}$ | ± | 0.26 | $1.27^{b}$ | ± | 0.19 | $0.51^{b}$ | ± | 0.09 | $0.78^{b}$ | ± | 0.26 | $1.25^{b}$ | ± | 0.32 |
| | 0.1-0.2 | $0.28^{b}$ | ± | 0.07 | $2.59^{a}$ | ± | 0.64 | $0.50^{b}$ | ± | 0.16 | $0.76^{ab}$ | ± | 0.11 | $0.47^{b}$ | ± | 0.10 | $0.45^{b}$ | ± | 0.09 | $0.70^{b}$ | ± | 0.17 |
| | 0.2-0.3 | $0.29^{b}$ | ± | 0.05 | $1.78^{a}$ | ± | 0.57 | $0.26^{b}$ | ± | 0.05 | $0.42^{b}$ | ± | 0.06 | $0.39^{b}$ | ± | 0.12 | $0.37^{b}$ | ± | 0.05 | $0.74^{ab}$ | ± | 0.20 |
| Specific root surface area ($m^2$ $kg^{-1}$) | 0-0.1 | $10.29^{c}$ | ± | 1.87 | $19.40^{a}$ | ± | 0.41 | $16.97^{ab}$ | ± | 1.73 | $11.14^{bc}$ | ± | 0.78 | $11.58^{bc}$ | ± | 0.60 | $14.32^{abc}$ | ± | 1.36 | $14.90^{abc}$ | ± | 1.47 |
| | 0.1-0.2 | $10.80^{b}$ | ± | 0.68 | $21.13^{a}$ | ± | 0.89 | $15.60^{ab}$ | ± | 1.96 | $10.17^{b}$ | ± | 0.36 | $11.59^{b}$ | ± | 1.28 | $13.74^{b}$ | ± | 2.74 | $13.17^{b}$ | ± | 0.66 |
| | 0.2-0.3 | $9.95^{cd}$ | ± | 0.70 | $20.15^{a}$ | ± | 1.30 | $15.92^{ab}$ | ± | 1.69 | $9.50^{d}$ | ± | 0.60 | $11.68^{bcd}$ | ± | 0.94 | $14.15^{abc}$ | ± | 0.85 | $11.92^{bcd}$ | ± | 1.27 |
| Root length density (cm $cm^{-3}$) | 0-0.1 | $0.70^{b}$ | ± | 0.24 | $6.56^{a}$ | ± | 0.65 | $1.51^{b}$ | ± | 0.42 | $1.70^{b}$ | ± | 0.33 | $0.57^{b}$ | ± | 0.07 | $1.03^{b}$ | ± | 0.27 | $1.82^{b}$ | ± | 0.43 |
| | 0.1-0.2 | $0.21^{c}$ | ± | 0.05 | $2.42^{a}$ | ± | 0.60 | $0.72^{b}$ | ± | 0.19 | $0.94^{ab}$ | ± | 0.15 | $0.43^{bc}$ | ± | 0.07 | $0.61^{b}$ | ± | 0.10 | $0.96^{ab}$ | ± | 0.20 |
| | 0.2-0.3 | $0.19^{c}$ | ± | 0.04 | $1.55^{a}$ | ± | 0.47 | $0.37^{bc}$ | ± | 0.06 | $0.46^{bc}$ | ± | 0.05 | $0.33^{bc}$ | ± | 0.07 | $0.48^{bc}$ | ± | 0.09 | $0.77^{ab}$ | ± | 0.19 |
| Root tip density (x $10^2$ $m^{-2}$) | 0-0.1 | $242.89^{bc}$ | ± | 45.28 | $1275.01^{a}$ | ± | 199.30 | $515.07^{abc}$ | ± | 127.84 | $625.53^{ab}$ | ± | 150.04 | $174.35^{c}$ | ± | 17.17 | $348.08^{bc}$ | ± | 88.43 | $528.29^{ab}$ | ± | 116.41 |
| | 0.1-0.2 | $63.31^{c}$ | ± | 11.36 | $512.43^{a}$ | ± | 132.38 | $260.47^{ab}$ | ± | 64.56 | $307.72^{a}$ | ± | 23.23 | $104.35^{bc}$ | ± | 14.62 | $205.66^{ab}$ | ± | 39.54 | $246.19^{ab}$ | ± | 36.84 |
| | 0.2-0.3 | $59.83^{c}$ | ± | 9.99 | $314.58^{a}$ | ± | 84.47 | $130.93^{abc}$ | ± | 17.09 | $137.32^{ab}$ | ± | 12.12 | $85.35^{bc}$ | ± | 16.00 | $157.04^{ab}$ | ± | 25.09 | $205.31^{a}$ | ± | 38.81 |

640

641

642 **Table 6.** Main effects of four contrasting soil textures' (Rendzic Leptosol, silty-clay loam – limestone
643 rich; Haplic Luvisol, silty-clay loam; Dystric Fluvic Cambisol, sandy silt loam; Dystric Gleysol, clay loam)
644 fine root biomass in three soil depths (0-0.1, 0.1-0.2, 0.2-0.3 m).

| Factor | df | F | *p*-value |
|---|---|---|---|
| Depth | 2 | 24.107 | 0.000 |
| Soil class | 3 | 6.394 | 0.002 |
| Depth*Class | 6 | 1.185 | 0.347 |

645 **Figure legends**

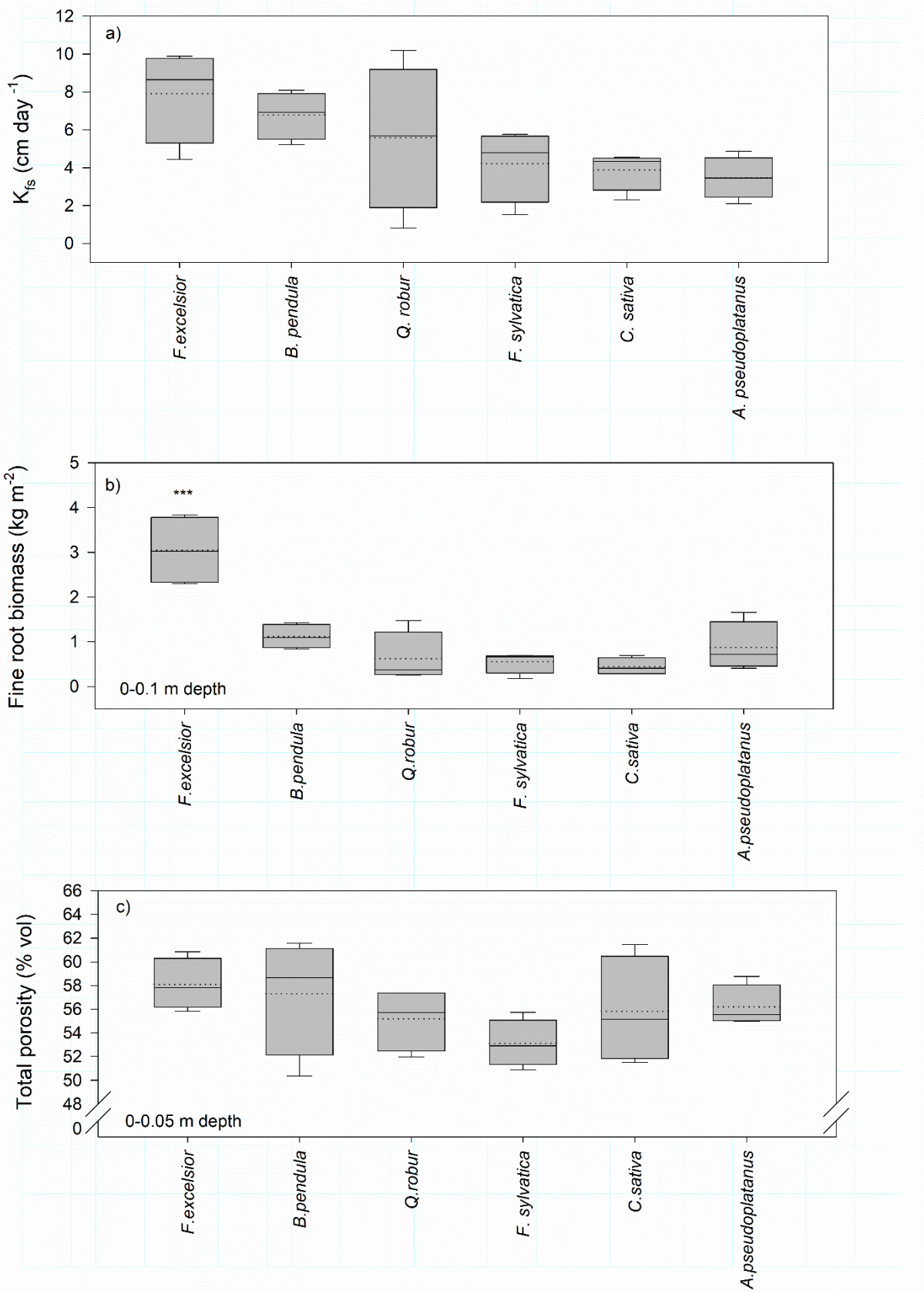


646

647 **Fig. 1**. Variation in soil and fine root properties amongst plots (n=4) of six tree species: (a) Surface field

648 saturated hydraulic conductivity ($K_{fs}$; cm day$^{-1}$), (b) fine root biomass (kg m$^{-2}$) in the 0-0.1 m depth, (c)

649 total soil porosity (% volume) calculated from cores (excluding stone fraction) taken from the 0-0.05
650 m depth. Data shown are mean (dashed horizontal line) and median (solid horizontal line). The boxes
651 define quartiles and whiskers ± one standard error. For fine root biomass, there was a species main
652 effect $p < 0.001$. No statistically significant differences were found in $K_{fs}$ or total porosity amongst
653 species ($p > 0.05$). *Alnus glutinosa* is excluded from biomass analysis because the stand was in poor
654 health, demonstrated by a large fraction of necromass amongst the fine roots.

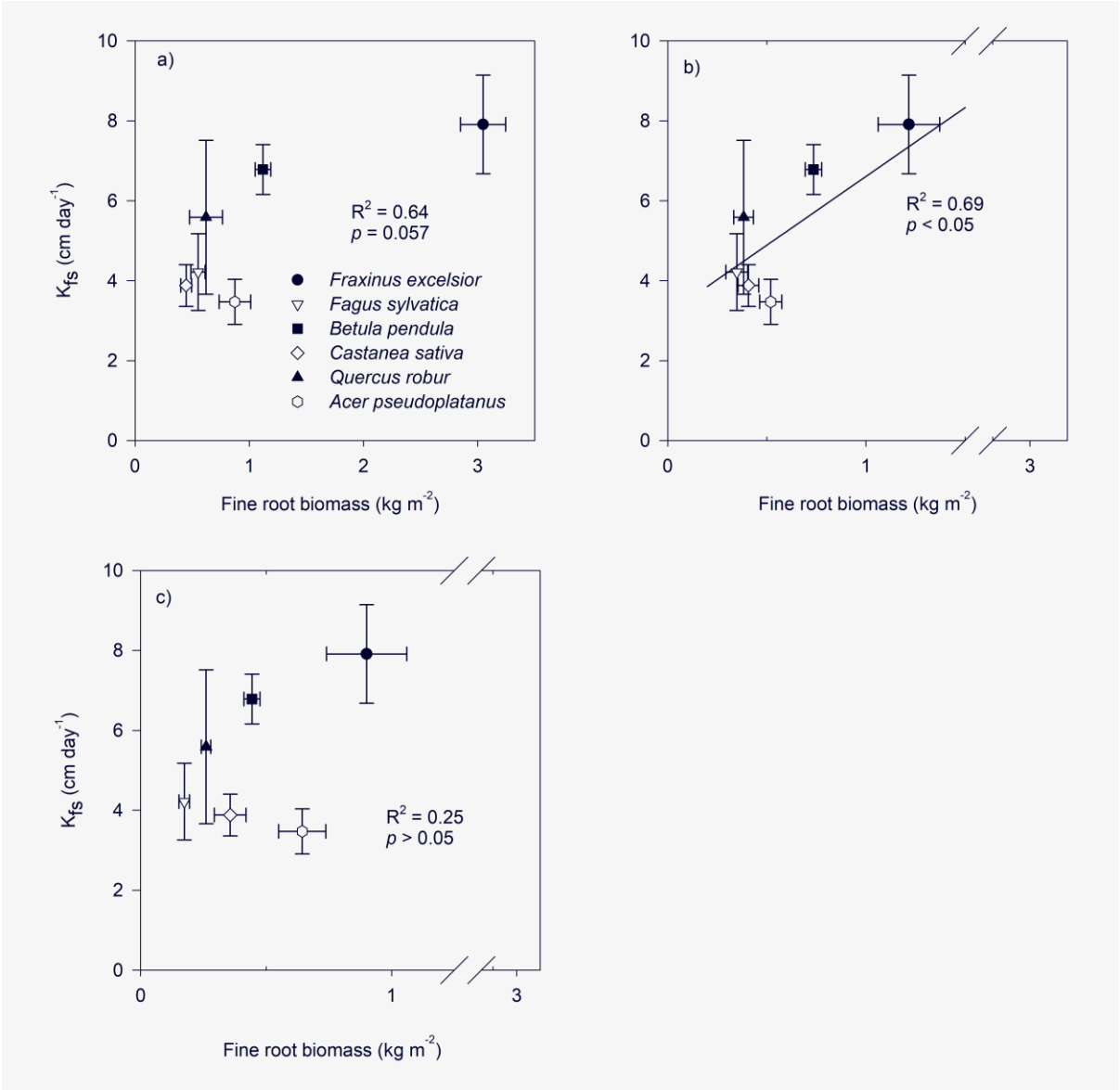


655

656 **Fig. 2**. Relationship between mean plot (n=4) surface field-saturated hydraulic conductivity ($K_{fs}$; cm
657 day$^{-1}$) and fine root biomass (kg m$^{-2}$) for six species, *F. excelsior, F. sylvatica, B. pendula, C. sativa, Q.*

*robur* and *A. pseudoplatanus*, in the (a) 0-0.1 m, (b) 0.1-0.2 m and (c) 0.2-0.3 m soil depths. Data shown are mean ± one standard error for each species. *Alnus glutinosa* is excluded from biomass analysis because the stand was in poor health, demonstrated by a large fraction of necromass amongst the fine roots.

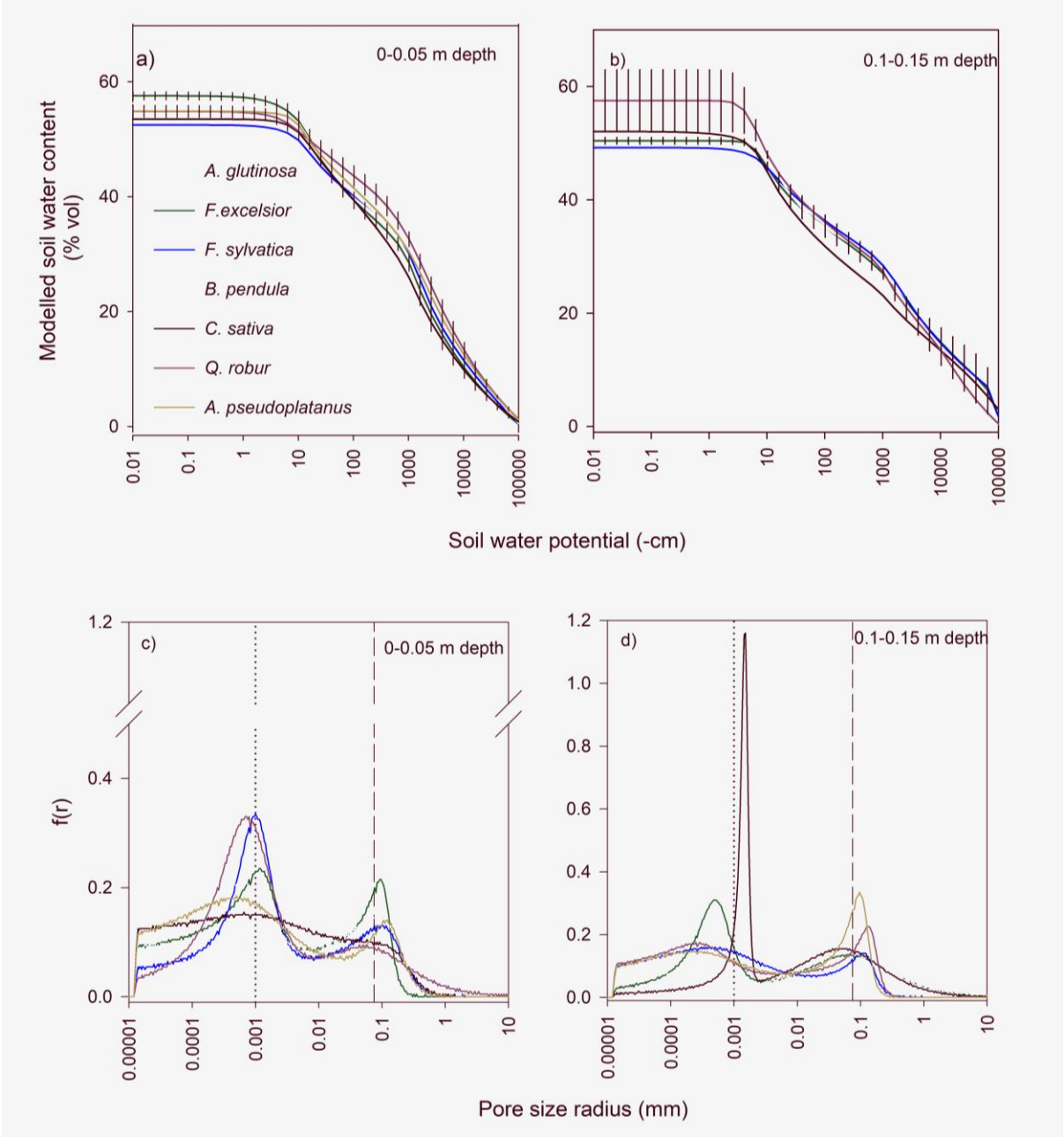


**Fig. 3**. Mean soil water retention curves for plots (n=4) of seven tree species in the (a) 0-0.05 m and (b) 0.01-0.15 m depths. The data are modelled using the bimodal Fredlund-Xing PDI model using

666 measured soil water content and potential (HYPROP) data. Modelled effective pore-size radius
667 distribution (Blonquist et al., 2006), displayed on a common log scale, of the seven species in the (c)
668 0-0.05 m and (d) 0.1-0.15 m depths. The pore-size distribution (f(r)) represents the proportional
669 volume of the combined effective pore size radii. Values to the right of the dotted vertical line indicate
670 pore radius sizes where capillary forces dominate water movement (Kosugi et al., 2002). Values to the
671 right of the dashed vertical line indicate macropore radius sizes > 0.075 mm.

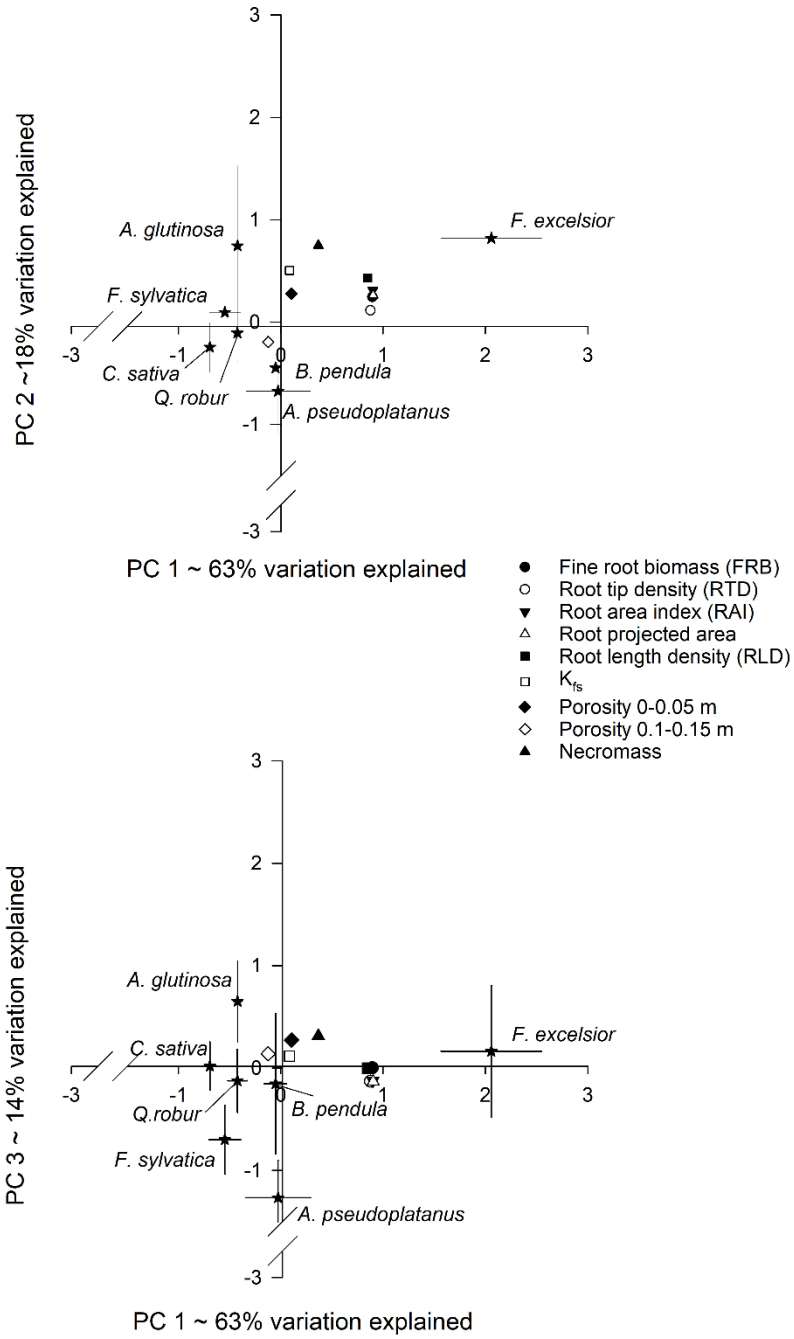


672

673 **Fig. 4**. Principal component analysis examining the relationships between field saturated hydraulic
674 conductivity ($K_{fs}$), tree species (*A. glutinosa, F. excelsior, B. pendula, F. sylvatica, C. sativa, Q. robur* and
675 *A. pseudoplatanus*), fine root morphological variables (root biomass, root tip number, root area index,
676 root projected area, root length density and necromass) and soil porosity (% volume) at two soil
677 depths (0-0.05 and 0.1-0.15 m). Error bars represent ± one standard error.

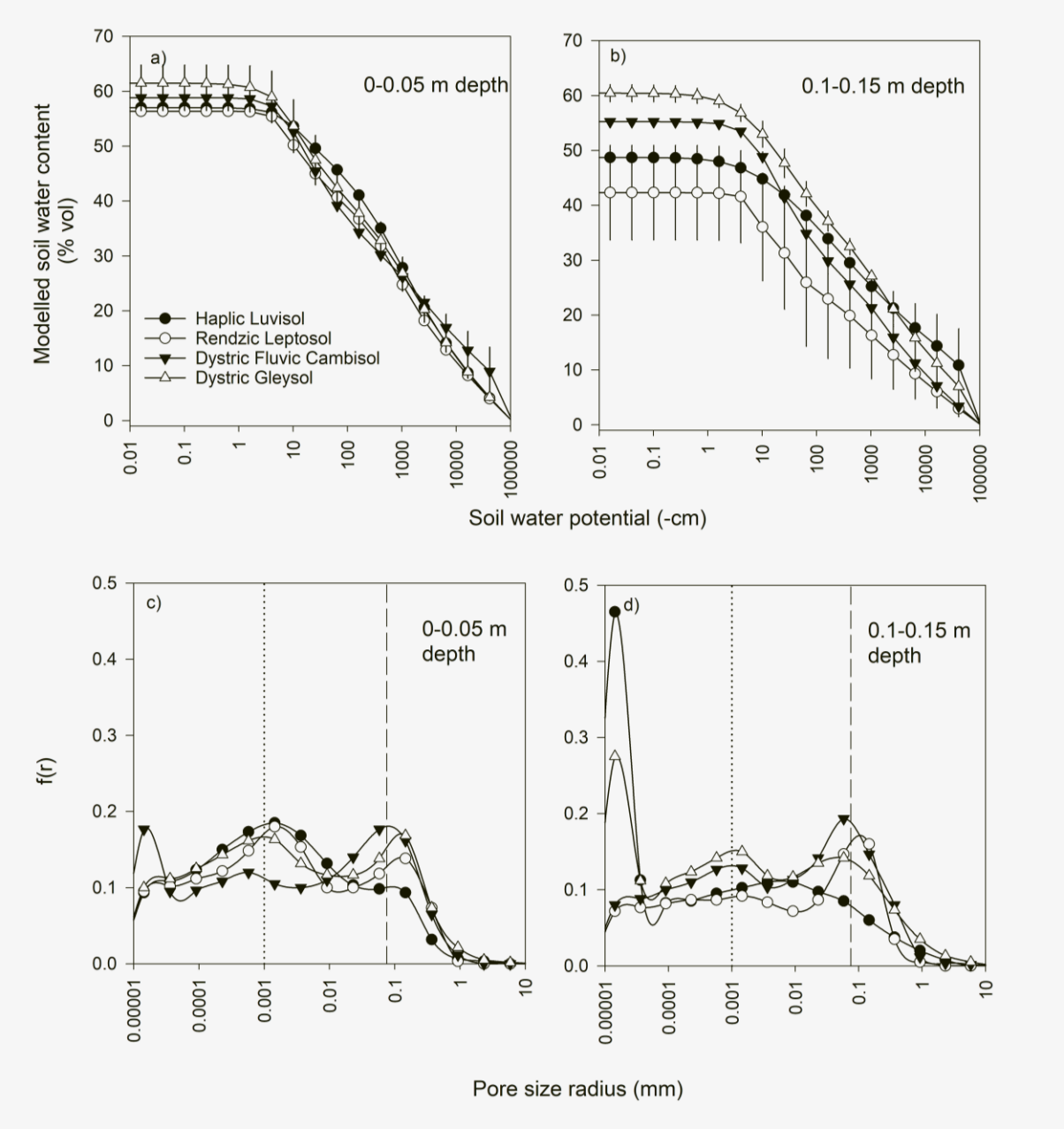


678

679 **Fig. 5**. Mean soil water retention curves for four sites with contrasting soil classes: Haplic Luvisol (silty
680 clay loam); Rendzic Leptosol (silty clay loam - limestone rich); Dystric Fluvic Cambisol (sandy silt loam);
681 and Dystric Gleysol (clay loam), at (a) 0-0.05 m and (b) 0.01-0.15 m depths. The data are modelled
682 using the bimodal Fredlund-Xing PDI model (Fredlund and Xing, 1994) using measured soil water
683 content (HYPROP) data. Modelled pore-size distribution (Blonquist et al., 2006) displayed on a
684 common log scale from contrasting soil classes at (c) 0-0.05 m and (d) 0.1-0.15 m depths. The pore-
685 size distribution (f(r)) represents the proportional volume of the combined effective pore size radii.

686 Values to the right of the dotted vertical line indicate pore sizes where capillary forces dominate water
687 movement (Kosugi et al., 2002). Values to the right of the dashed vertical line indicate macropore pore
688 sizes > 0.075 mm. Values between the vertical lines indicate mesopores.

689

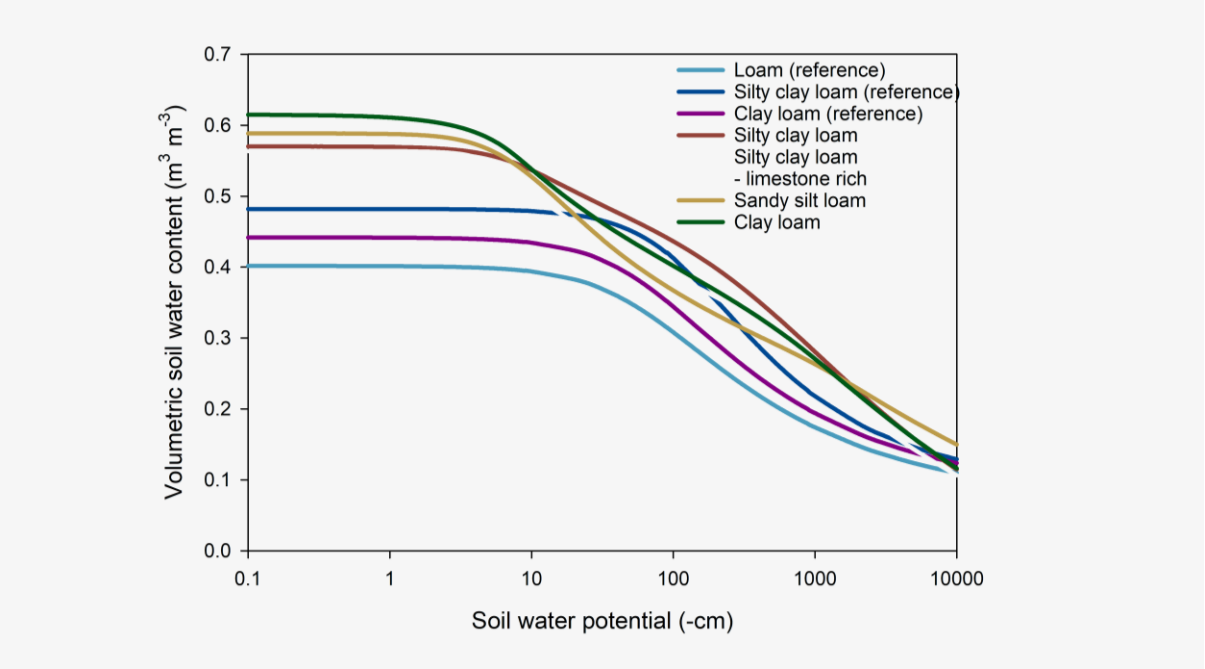


690

691 **Fig. 6.** Soil water retention curves (SWRC) for the four soil textures used in our study: Haplic Luvisol
692 (silty clay loam); Rendzic Leptosol (silty clay loam - limestone rich); Dystric Fluvic Cambisol (sandy silt
693 loam); and Dystric Gleysol (clay loam), and modelled SWRC for three reference soil textures (loam,
694 silty clay loam and clay loam) from the Rosetta modelling framework for pedotransfer functions
695 (Schaap et al., 2001). pF, the decimal log of soil water potential (cm), describes the amount of force
696 or suction required to extract water from the soil.